A Realistic Path Loss Model for Cell-Free Massive MIMO in Urban Environments

Thomas Choi*, Issei Kanno†, Masaaki Ito†, Wei-Yu Chen* and Andreas F. Molisch*
*University of Southern California, Los Angeles, United States
†KDDI Research, Inc., Saitama, Japan

GLOBECOM 2022 - 2022 IEEE Global Communications Conference | 978-1-6654-3540-6/22/$31.00 ©2022 IEEE | DOI: 10.1109/GLOBECOM48099.2022.10001398

***Abstract*—Cell-free massive multi-input multi-output (CF-mMIMO) systems are one of the key technologies for 6G. Currently, performance assessment of such systems is hampered by the fact that there are no specific path loss (PL) models for CF-mMIMO. Conventional PL models based on Euclidean distance and log-normal shadowing assuming spatial stationarity across coverage area are usually employed for simplicity but show significant deviations from reality particularly in urban environments, which are the main deployment scenario for CF-mMIMO. In this work, we provide the first realistic channel model for CF-mMIMO systems in urban environments, introducing non-isotropic, non-stationary behavior in different parts of street canyon locations and incorporating both correlations between access points, and between user equipments. Simulation results demonstrate the superior reproduction of typical PL values in urban street canyons.**

***Index Terms*—Cell-free (distributed) massive MIMO, channel modeling, path loss, propagation, ray tracing**

I. Introduction

A. Motivation

Cell-free massive multi-input multi-output (CF-mMIMO), which distributes antennas of a base station (BS) to many different locations (access points, APs) within a large coverage area to serve a large number of user equipments (UEs), is regarded as one of the key potential technologies for 6G [1]–[3].[1] As a UE is likely to be near at least one AP, CF-mMIMO provides macro-diversity, resulting in uniform user experience regardless of the UE location within the coverage area, and since signals to/from different APs are jointly processed, the inter-cell interference normally experienced by cellular systems is avoided.

Realistic path loss (PL) information is very important for evaluating performances of CF-mMIMO systems, as it can help determine optimal spatial density of APs, number of antennas per AP, UE assignment algorithms, etc. Most previous CF-mMIMO works have employed simple PL models based on Euclidean distances between APs and UEs combined with log-normal shadowing assuming spatial stationarity across a coverage area. However, such a model is not realistic for urban environments (the most important scenario for CF-mMIMO deployment), as different streets show non-isotropic, non-stationary PL behaviors due to different propagation characteristics. For example, Fig. 1 shows that data generated from a traditional PL model deviate significantly from data obtained from ray tracing in the same environment.

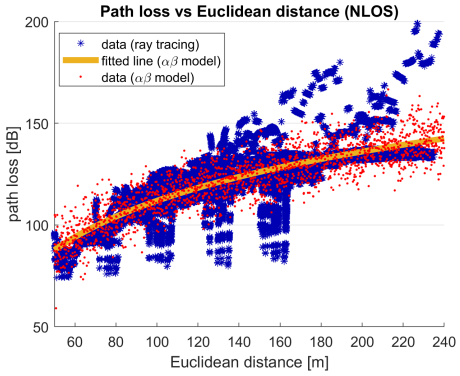

Fig. 1. PL versus Euclidean distance of all non-line-of-sight (NLOS) data in Sec. IV are shown, along with a best-fitted line and generated data based on statistical parameters of the $\alpha\beta$ model.

The main source of this discrepancy is that traditional models consider PL to be dependent only on the Euclidean distance between transmitter (TX) and receiver (RX), and thus isotropic (i.e., the same in all directions) and stationary (independent of the starting location). However, in urban environments, the connections to the different APs are mostly governed by the waveguiding processes that very distinctly depend on parameters other than Euclidean distance. Thus, for CF-mMIMO, a new modeling approach is required.

B. Related works

Several works have modeled the PL as a function of the Manhattan (instead of Euclidean) distance [4]–[6], but the obtained parameters were deterministic (partly incorporating street shapes). Most related to this paper is our own previous work suggesting a street-by-street model with probabilistic parameters [7], [8] at millimeter wave frequencies. However, in all of these cases, the focus was on the propagation from a BS to multiple UEs (or, equivalently, to a UE on a trajectory), i.e., the classical cellular case, and thus does not cover CF-mMIMO scenarios. Correlations of shadowing between signals to/from multiple BSs, as well as 3D multipath channel models including the correlations based on angles [9] and common clusters of scatterers [10] have been discussed,

This work was financially supported by KDDI Research, Inc. and the National Science Foundation under grant no. ECCS-1731694.

[1]Cell-free massive MIMO stems from other technologies such as distributed MIMO, network MIMO, cooperative multi-point (CoMP), ultra-dense networks, etc., but employs principles and algorithms of massive MIMO (e.g., high ratio of BS antennas to UEs and linear processing).

but the discussion does not extend to parameters of the street canyon environments.

Conversely, several types of channel models were suggested for CF-mMIMO system analysis, such as probabilistic line-of-sight (LOS) model [11] and correlated Rayleigh/Rician models [12], [13]; however, in none of those are the specifics of street environments considered. Generally, CF-mMIMO system analysis is still based on the assumption of isotropic stationary channels. Thus, in summary, we find that no sufficiently realistic model is currently available for simulating CF-mMIMO in urban environments.

C. Contribution

To close this gap, in this work, we propose a realistic channel model for CF-mMIMO systems in urban environments, incorporating the non-isotropy and non-stationarity of PL and shadowing, as well as the correlation of PL and other channel parameters both between the links of one UE to the different APs, and between the AP and multiple UEs; we name this model CUNEC (Cell-free massive mimo for Urban Non-stationary Environment with Correlations). Specifically, our contributions include

- A generic modeling approach incorporating the specifics of propagation in urban street canyons, including waveguiding, diffraction around street corners, and over-the-rooftop propagation.
- Incorporation of the random variations between streets, and the non-isotropic, non-stationary nature of PL and shadowing.
- Incorporation of both the UE-to-multiple-APs, and the AP-to-multiple-UEs link correlations.
- Parameterization of the model from ray tracing results.
- Verification (based on ray tracing) that the model works well even when environmental parameters are varied.

Overall, we show that our model is significantly better at estimating and emulating the PL between the APs and UEs for CF-mMIMO systems than a conventional model, which does not take the propagation environment into account.

II. Path loss definition and conventional model

A. Definitions and nomenclature

The ratio of the transmit power to the receive power is defined as the sum (on a dB scale) of a (i) distance-dependent "expected" PL (represented by $\overline{PL}$), (ii) large-scale fading (represented by shadowing S), and (iii) small-scale fading. Small-scale fading can be averaged out over multiple realizations, e.g., locations within a small area. In the following, we denote the locations of the AP and UE as $\mathbf{r}_{\mathrm{AP}}$ and $\mathbf{r}_{\mathrm{UE}}$, respectively, and define $d = |\mathbf{r}_{\mathrm{AP}} - \mathbf{r}_{\mathrm{UE}}|$ as the distance between AP and UE. With this notation established, we can now write

$$PL(\mathbf{r}_{\mathrm{AP}}, \mathbf{r}_{\mathrm{UE}}) = \overline{PL}(\mathbf{r}_{\mathrm{AP}}, \mathbf{r}_{\mathrm{UE}}) + S(\mathbf{r}_{\mathrm{AP}}, \mathbf{r}_{\mathrm{UE}}). \quad (1)$$

This is the most general form. It is *a common assumption, which might not be fulfilled in urban environments,* that $\overline{PL}$ and S are stationary and can be modeled as depending only on d. For S, the autocorrelation function is often assumed to be exponentially distributed with $\rho_{SS}(d_{corr}) = 1/e$ where d_{corr} is the correlation distance.

In the following, we first review the common power-law (also known as $\alpha\beta$) model combined with log-normal shadowing. We then describe the CUNEC PL model that we propose.

B. $\alpha\beta$ model with log-normal fading

The by far most common channel model is the $\alpha\beta$ model, which assumes that $\overline{PL}$ and S depend only on distance d, and then assumes (on a double-logarithmic scale) a straight line fit

$$\overline{PL}_{\alpha\beta}(d) = 10 \cdot \alpha \cdot \log_{10}(d/d_0) + \beta, \quad (2)$$

where α is the slope of the line (also known as a PL exponent), d_0 is the arbitrarily chosen reference distance, and β is the offset value which is the PL at d_0.

Then, the overall PL, $PL_{\alpha\beta}$, is generated by:

$$PL_{\alpha\beta}(d) = \overline{PL}_{\alpha\beta}(d) + \mathcal{N}(0, \sigma_S), \quad (3)$$

where σ_S is the shadowing standard deviation (SD) calculated as the variations of the $\overline{PL}_{\alpha\beta}$ over the existing "to-be-modeled" PL data assuming normal distribution. σ_S is usually calculated separately for LOS and NLOS scenarios. This approach has been used for conventional cellular systems, as well as wireless LANs and other systems, for more than 50 years, from the Okumura-Hata model to the current 3GPP standards.

III. The CUNEC model

As discussed in Sec. I, the fundamental idea of the CUNEC model is to account for (i) different propagation effects in different "orders" of streets (number of "turn the corner" between AP and UE), (ii) random variations of PL exponents even between streets of the same type, (iii) impact of different "starting points" for the PL computations (i.e., nonstationarities), (iv) over-the-rooftop propagation, which may prevent the PL to depend only on a simple Manhattan distances, and (v) nonstationarities of the shadowing.

When considering the propagation from a UE to different APs, we note that some APs are in the same street canyon ("zero-order" streets), providing a LOS (or obstructed LOS) connection, while others are in streets that intersect the street of the UE at an angle, thus giving rise to NLOS situations, which require any multipath components (MPCs) to be diffracted, or reflected multiple times, to reach the AP. We note that in general, APs can also be in streets parallel to that of the UE ("second-order" streets), though the PL to those is generally very high.

1) Zero-order streets: For the zero-order streets, i.e., LOS scenarios, the CUNEC model is similar to the $\alpha\beta$ model in that PL depends essentially on the Euclidean distance. However, in contrast to the standard $\alpha\beta$ model, we consider variations of α and β across different streets. The collection of parameter values of all LOS streets is modeled as an ensemble of realizations of random variables, with the correlations among

the parameters considered. In other words, the PL at one LOS street is modeled as:

$$\begin{aligned}\overline{PL}_{LOS}(d) &= 10 \cdot \alpha_{LOS} \cdot \log_{10}(d/d_0) + \beta_{LOS} \\ &= 10 \cdot \alpha_{LOS} \cdot \log_{10}(d/1\mathrm{m}) + FSPL_{1\mathrm{m}} + \Delta_{LOS}\end{aligned} \quad (4)$$

where $FSPL_{1\mathrm{m}}$ is the expected free space PL at 1m (at 3.5 GHz in this paper) and Δ_{LOS} is the offset of the best fitting line. There will be different values of α_{LOS} and Δ_{LOS} for different streets. Similarly, shadowing SD σ_{S-LOS} and correlation distance $d_{corr-LOS}$ are considered a random variable, though we assume them to be independent of d (this latter assumption can be relaxed easily within the framework of our model); thus, shadowing is not stationary but dependent of the street the UE is located in. Besides the usual sources of large-scale variations, such as variations of the reflection coefficients of buildings, obstructions of the LOS by trees, lantern masts, etc., can be considered.

2) First-order streets (NLOS1): NLOS1 indicates that there is no LOS and the signal between an AP and a UE needs to turn at least one building corner. The PL value then becomes the PL from the TX to the corner plus the corner loss plus the PL after turning the corner, with an extra term describing transition between LOS and NLOS1. The PL equation for the NLOS1 is then:

$$\begin{aligned}\overline{PL}_{NLOS1} = \overline{PL}_{LOS}(d_{n1}) + \frac{\Delta_{NLOS1} \cdot {d_a}^2}{\kappa(d_t)^2 + {d_a}^2} \\ + 10 \cdot \alpha_{NLOS1} \cdot \log_{10}(d_a/1\mathrm{m}),\end{aligned} \quad (5)$$

where d_{n1} is the distance between the TX and the corner nearest to the RX, Δ_{NLOS1} is the corner loss, d_a is the additional distance from the corner to the RX, d_t is the distance between RX and the canyon (house) walls, $\kappa(d_t)$ will be discussed below and α_{NLOS1} is the PL exponent of the street between the corner and the RX.

The second term in (5) describes the corner loss. While in the millimeter wave model of [8] it was simply represented as a constant, we here describe it as a function that ensures a smooth transition from LOS to NLOS 1. The functional form, parameterized by $\kappa(d_t)$, describes a saturation behavior, and the speed of saturation depends on how far the RX is away from the corner, both parallel (indicated by d_a) and perpendicular (indicated by d_t) to the signal path. The term indicates that the corner loss term eventually saturates to Δ_{NLOS1} which physically indicates that the corner loss becomes a constant when the RX is far from the corner. Note that Δ_{NLOS1} may depend on the angle between the two intersecting streets. While in this paper we consider only right-angle intersections, more general modeling is important in particular in older cities where streets may intersect at almost any angle. Finally, we note that the parameters can depend on the distance of the TX to the corner. This dependence can be seen as random (i.e., contributing to the ensemble of parameter values in the random environment), or it could be described deterministically, as impacting the value of Δ_{NLOS1} and α_{NLOS1}. In order not to make the model overly complicated, we choose here the former option; this has, however, implications for the modeling of the correlation of different APs and UEs.

In addition to the waveguiding described above, over-the-rooftop propagation can be of significant importance in CF-mMIMO. It can be considered to be mostly independent of the waveguiding (as confirmed by preliminary ray tracing analysis), so that the overall PL ($\overline{PL}_{tot}$) can be computed as

$$\frac{1}{\overline{PL}_{tot}} = \frac{1}{\overline{PL}_{otr}} + \frac{1}{\overline{PL}_{NLOS1}} \quad (6)$$

where the over-the-rooftop PL ($\overline{PL}_{otr}$) can be modeled, e.g., by the well-known COST231 Walfish-Ikegami model [14]. The same approach can be applied for all higher-order streets.

3) Second-order streets (NLOS2): NLOS2 indicates that there are at least two corners between the AP and the UE. The PL up to the second corner is calculated by PL_{NLOS1} equation, and the distance-based PL term is added as:

$$\begin{aligned}\overline{PL}_{NLOS2} = \overline{PL}_{NLOS1}(d_{n2}) + \\ 10 \cdot \alpha_{NLOS2} \cdot \log_{10}(d_a/1\mathrm{m}) + \Delta_{NLOS2},\end{aligned} \quad (7)$$

where d_{n2} is the Manhattan distance up to the second corner, α_{NLOS2} is the PL exponent of the street after the second corner is turned, and Δ_{NLOS2} is the corner loss of the second corner. Compared to the corner turning into first-order streets, the additional loss shows a less pronounced saturating behavior; furthermore second-order (and higher-order streets) generally shows high PL and are thus of less practical importance; thus the simpler model (7) was chosen instead of using a saturation function as in (5).

4) Correlation between different UEs: The above sections describe the PL between a single UE and multiple APs located in different streets. However, the correlation between the channels from these APs to multiple UEs (or a single UE on a trajectory) also needs to be described. This behavior is modeled implicitly in our approach. It is, however, noteworthy that the PL from different UE locations in the same street, to a given set of APs, experiences *different* PL parameters, as confirmed by our ray tracing simulations. UE displacement also leads to different shadowing realizations, which leads to a decorrelation in addition to the decorrelation experienced at different AP locations. Since correlations between different UEs has been explored more extensively in the literature, we do not consider it in the remainder of this paper and defer to future work [15].

IV. Ray tracing simulation

In order to obtain model parameters and test model performances, we used ray tracing simulation based on Wireless Insite software from Remcom. Ray tracing is especially useful to generate a controlled environment, minimizing the unknowns and allowing direct physical interpretation of the ray propagation.

To test different types of modeling methodologies, we simulated a simple Manhattan structure 4×4 buildings whose length, width, and height varied between 25m and 45m and the

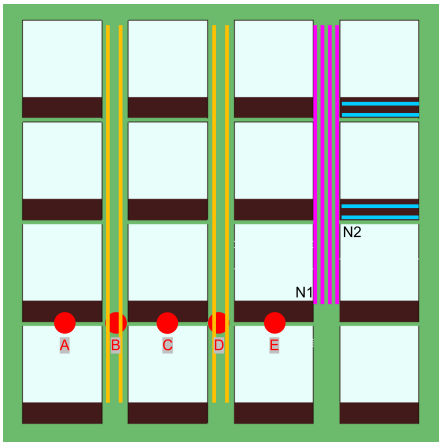

Fig. 2. One of the ray tracing scenarios with 4×4 buildings is shown (brown parts indicates walls of buildings). Each building has a dimension of either 45m or 25m length/width/height (separate simulations). The buildings are separated 15m or 5m apart. UEs on ground are indicated by red dots, and AP trajectories (collection of potential AP locations) located near the rooftops at 45m or 25m height by color lines, with the color indicating street order.

streetwidth varied between 5m and 15m, shown in Fig. 2. UEs are modeled as TXs on ground, while APs are RXs at 45m height each placed 0.05m apart, forming what is commonly called in ray tracing "trajectories", although of course APs do not move. These trajectories are parallel to the canyon walls. We note that for most deployments, the APs will be located on the building walls, below or at rooftop heights; however, for some situations such as high lantern masts, APs with an offset from the building walls are possible as well, and are thus included in our modeling. The number of MPCs is limited to 40, the number of reflections per MPC is limited to 30, and the number of diffractions per MPC is limited to 1.

V. Path Loss Model Parameters

The PL model parameters for the $\alpha\beta$ model and the CUNEC model are obtained from the ray tracing data in Sec. IV. Due to space constraints, we here (i) do not include over-the-rooftop components and (ii) do not consider in detail the correlations between different UE positions. Those will be reported in [15].

A. Line-of-sight (LOS)

For the $\alpha\beta$ model, all PL values obtained from all LOS trajectories are first plotted together against the distances between the UEs and APs within the trajectories, to find a single set of PL parameters representing all data (Sec. II-B), as shown in first column of Table I.[2][3] For the CUNEC model, we find a set of parameters per UE/AP combination (Sec. III), and calculate the statistics and correlations of all collected parameters, as shown in Table I and Table II.

The results from Table I show that for the LOS scenario, parameter values from the $\alpha\beta$ model and means of parameter values from the CUNEC model are close (both average over all available LOS points, though with slightly different mechanisms). The SD of the α is relatively small; the reasons for that are (i) the dominant signal path, which is the direct path in the LOS scenario, has a small variance in terms of channel gain and (ii) the ray tracing scenario is simple and symmetric. Still, the CUNEC model has less shadowing SD (1.25 dB) than the $\alpha\beta$ model (1.96 dB), indicating a better fitting of the data within each street.

TABLE I
Parameter values for LOS

	$\alpha\beta$	CUNEC (mean)	CUNEC (SD)
α	1.312	1.361	0.258
Δ	6.948	6.115	5.036
σ_S	1.963	1.247	0.329
d_{corr}	-	11.54	3.705

TABLE II
Correlations of CUNEC LOS parameters

	α	Δ	σ_S
Δ	**-0.940**		
σ_S	0.029	-0.316	
d_{corr}	-0.392	0.200	**0.606**

The results from Table II shows that the correlation occurs for two pairs of parameters.[4] α and Δ are highly correlated, indicating that the relatively low PL exponent (α: 1.3-1.4) is compensated by some offset value (Δ: 6-7 dB) in comparison to the usual free space PL equation with higher PL exponent value ($\alpha = 2$). There are some correlations among shadowing SD and correlation distance as well.

B. Non-line-of-sight one corner (NLOS1)

For the $\alpha\beta$ model, all PL values obtained from all NLOS trajectories (no distinction between NLOS1 and NLOS2, in accordance with common practice) are plotted against "Euclidean" distances and the PL parameters are fitted.

For the CUNEC model, and first-order streets, the APs that are one corner away from the UEs are chosen to obtain the channel parameters, such as pink AP trajectories in Fig. 2 with corner "N1".[5] For example, Fig. 3 shows the additional PL from the corner N1 to the APs on one of the pink trajectories for three UEs (A, C, and E).[6]

[2]We assume the reference distance is 1m for the $\alpha\beta$ model as well to find the offset $\Delta = \beta - FSPL_{1\text{m}}$ instead of β.

[3]d_{corr} is skipped for the $\alpha\beta$ model, as finding d_{corr} from data collected over many trajectories is not straightforward.

[4]We assume two parameters are correlated if the magnitude of the correlation is in between 0.5 and 1.

[5]To find the values of parameters for the NLOS1 model, we use an iterative approach. Parameter α is first found from the shallower slopes of the curves when the additional distance from corner d_a is large and the UEs are farther away from the corner (this α is then fixed to a single value for APs located in the same line). After fixing the value of α, corner loss Δ is then found, which also must fit the shallower slopes of the curves well (this Δ also is fixed to a single value). Lastly, a set of κ which is different for all UEs is found to best fit the curves even for the steeper parts of the curves and UEs close to the corner.

[6]These data are obtained by subtracting the obtained PL values by the LOS PL values from the UEs to corner N1: $\overline{PL}_{NLOS1} - \overline{PL}_{LOS}(d_{n1})$.

TABLE III
PARAMETER VALUES FOR NLOS1 (FROM CORNER N1 FOR CUNEC)

	$\alpha\beta$	CUNEC (mean)	CUNEC (SD)
α	8.032	0.959	0.128
Δ	-92.06	34.83	2.778
σ_S	8.179	2.964	1.216
d_{corr}	-	4.716	2.621

TABLE IV
CORRELATIONS OF CUNEC NLOS1 PARAMETERS

	α	Δ	κ	σ_S	d_{corr}
Δ	**-0.920**				
κ	0.116	-0.074			
σ_S	-0.234	0.236	0.281		
d_{corr}	0.047	-0.163	0.194	0.056	
d_n	-0.043	0.018	**-0.852**	**-0.560**	-0.293
d_t	**0.604**	**-0.694**	0.065	-0.463	0.191

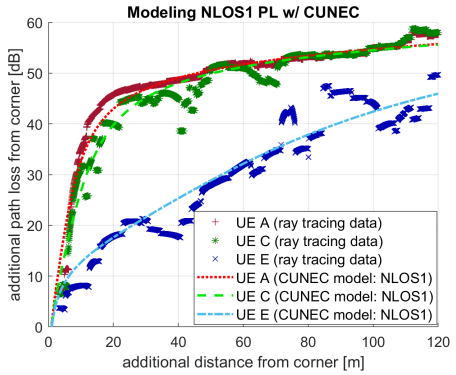

Fig. 3. Additional PL from corner N1 (ray tracing data and fitted lines using mean parameter values from the CUNEC model) for one of the NLOS1 scenario (one of pink AP trajectories and three UEs: A, C, and E, in Fig. 2) is plotted against d_a. The parameters for the CUNEC model are collected for each combination of UE and trajectory of APs.

As we can see visually from Fig. 1 and Fig. 3 as well as by comparing the shadowing SD in Table III, the CUNEC model fits the ray tracing data much better than the $\alpha\beta$ model. In addition, the parameter values of the $\alpha\beta$ model may be misleading if the NLOS PL data are obtained from a specific environment; the best-fitting line for all NLOS1 data has an unusually high α value and negative Δ value, which do not make physical sense. In comparison, the CUNEC model provides parameter values which can be interpreted physically; the PL quickly increases as the signal turns the corner and reaches up to 35 dB of corner loss (Δ) when the AP is deep in the cross street from the UE.

Again, the statistics and correlations of all collected parameters are shown in Table III and Table IV, where additional parameters such as the saturation constant κ, distance to corner, d_c, and corner to street trajectory length, d_t, are also considered for correlation analysis. In the NLOS1 scenario, the α and Δ are highly correlated, as in the LOS scenario. Another highly correlated pairs of parameters are, of course, the distance to corner d_n and saturation constant κ, as the κ in (5) is likely to be low (saturates fast) if the UE-corner distance is large and vice-versa, as shown in Fig. 3. Corner distance d_n is also weakly negatively correlated with shadowing SD. Likewise, the distance from the corner to the closest point of the NLOS1 trajectory d_t is weakly correlated with α and Δ, indicating that higher value of α and lower value of Δ are expected when the AP is further away from the corner.

The parameters for second-order streets are extracted in a similar fashion; results are shown in Tables V and VI.

TABLE V
PARAMETER VALUES FOR NLOS2 (FROM CORNER N2 FOR CUNEC)

	$\alpha\beta$	CUNEC (mean)	CUNEC (SD)
α	8.032	1.652	0.556
Δ	-92.06	0.841	6.379
σ_S	8.179	4.660	1.477
d_{corr}	-	2.700	0.787

TABLE VI
CORRELATIONS OF CUNEC NLOS2 PARAMETERS

	α	Δ	σ_S
Δ	-0.039		
σ_S	**0.602**	0.482	
d_{corr}	0.328	-0.006	0.353

C. Correlation of UEs

We finally test whether the modeling methodology, and the parameter values of the CUNEC and $\alpha\beta$ models obtained from Sec. V, also correctly emulates the behavior of UEs moving on a trajectory. While not shown here for space reasons, the behavior of a moving UE could be well reproduced by our model, within roughly the same accuracy as that of multiple-AP links, without need for further parameterization. Examples will be provided in [15].

D. Verification tests

To verify the usefulness of our model, we simulate the resulting PL in a test scenario that is chosen to be similar to Sec. IV with same settings in number of MPCs, reflections, and diffractions, but with changes in building dimensions (length/width/height) and street width (set to 35m and 25m respectively). The LOS, NLOS1, and NLOS2 locations are included.

Fig. 5 shows the expected PL values of the CUNEC and $\alpha\beta$ models using the parameter values obtained versus the raw PL values from the ray tracing test scenario in Fig. 4. To avoid excessive cluttering of the figure, we are only showing the simulation results when all CUNEC parameters are chosen as their mean value.

The first observation is that the CUNEC model fits the ray tracing data much better than the $\alpha\beta$ model in NLOS situations. While the parameter values of the $\alpha\beta$ model are also derived from a similar environment as a test environment, the $\alpha\beta$ model overestimates the PL, indicating that the values of the parameters cannot be transferred from an environment

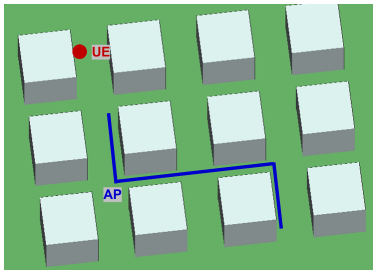

Fig. 4. Test environment with a single UE and APs on a line.

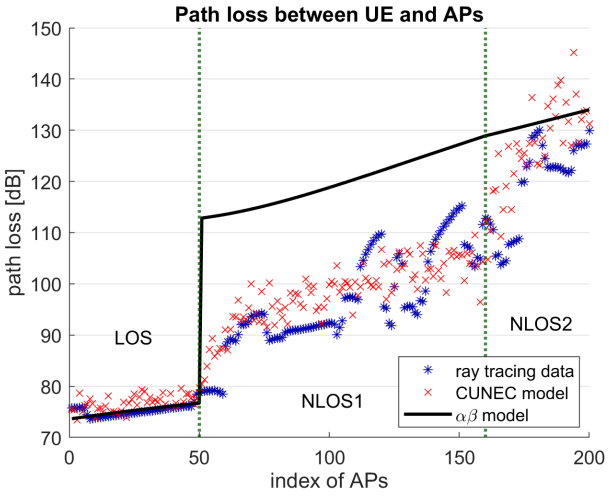

Fig. 5. PL values from ray tracing simulation in Fig. 4 and expected PL values using the model parameters versus indices of the AP.

and setup to another. Using an arbitrary value of spatially stationary σ_S value can result in inaccurate estimation of PL values, which can be critical for CF-mMIMO systems determining optimal deployment of the APs and clustering of APs for each UE [16]. The root-mean-square deviation of the CUNEC and the $\alpha\beta$ model are 6.26 dB and 11.3 dB respectively, showing significant, and practically relevant, differences in performance.

Another observation is that the $\alpha\beta$ model shows discontinuities of the PL values as we move from LOS to NLOS1 to NLOS2, while the CUNEC model shows smoother transitions. The $\alpha\beta$ model only varies the σ_S depending on LOS and NLOS, while the CUNEC model considers the PL value up to the nearest building corner as a starting point for PL estimation and considers the corner loss of the NLOS1 to be a saturation process, which is a more accurate description of signal propagation across street canyons. The CUNEC model also considers NLOS2 separately from NLOS1, obtaining accurate PL values even for deep shadowing scenarios. Overall, the CUNEC model provides more accurate PL values between an AP and a UE in a selected environment than the $\alpha\beta$ model.

VI. Conclusion

In this paper we proposed a novel channel model, which we term CUNEC, that can describe, in a realistic manner, PL and shadowing of CF-mMIMO systems in urban environments. The model explicitly considers the street canyon environment and the dominant propagation processes occurring in it. It avoids the common simplifications of PL models that are not fulfilled in urban street canyon environments, that PL and shadowing are isotropic and stationary. Such a realistic model is well suited for new wireless technologies like CF-mMIMO where the deployment strategies of the APs and clustering of APs for each UE in a selected environment are crucial.

In the future, we will consider correlations among different UEs as well as APs, over-the-rooftop propagation, simulation and parameterization in an environment with varying shapes of buildings, and verification of the model to real-world measurement data at 3.5 GHz.

References

[1] H. Tataria, M. Shafi, A. F. Molisch, M. Dohler, H. Sjöland, and F. Tufvesson, "6G wireless systems: vision, requirements, challenges, insights, and opportunities," *Proc. IEEE*, vol. 109, no. 7, pp. 1166–1199, 2021.

[2] H. Q. Ngo, A. Ashikhmin, H. Yang, E. G. Larsson, and T. L. Marzetta, "Cell-free massive MIMO versus small cells," *IEEE Trans. Wireless Commun.*, vol. 16, no. 3, pp. 1834–1850, 2017.

[3] Özlem Tugfe Demir, E. Björnson, and L. Sanguinetti, "Foundations of user-centric cell-free massive MIMO," *Found. and Trends Signal Process.*, vol. 14, no. 3-4, pp. 162–472, 2021.

[4] J.-E. Berg, "A recursive method for street microcell path loss calculations," in *Proc. 6th Int. Symp. Pers., Indoor, Mobile Radio Commun.*, vol. 1, 1995, pp. 140–143 vol.1.

[5] K. Haneda, N. Omaki, T. Imai, L. Raschkowski, M. Peter, and A. Roivainen, "Frequency-agile pathloss models for urban street canyons," *IEEE Trans. Antennas Propag.*, vol. 64, no. 5, pp. 1941–1951, 2016.

[6] 3GPP, "5G; study on channel model for frequencies from 0.5 to 100 GHz," 3rd Generation Partnership Project (3GPP), Technical Specification (TS) 3gpp.38.901, 11 2020, version 16.1.0.

[7] A. F. Molisch, A. Karttunen, S. Hur, J. Park, and J. Zhang, "Spatially consistent pathloss modeling for millimeter-wave channels in urban environments," in *2016 10th Eur. Conf. Antennas and Propag. (EuCAP)*, pp. 1–5.

[8] A. Karttunen, A. F. Molisch, S. Hur, J. Park, and C. J. Zhang, "Spatially consistent street-by-street path loss model for 28-GHz channels in micro cell urban environments," *IEEE Trans. Wireless Commun.*, vol. 16, no. 11, pp. 7538–7550, 2017.

[9] C. Liao, K. Xu, X. Xia, W. Xie, and M. Wang, "AOA-assisted fingerprint localization for cell-free massive MIMO system based on 3D multipath channel model," in *2020 IEEE 6th Int. Conf. Comput. and Commun. (ICCC)*, pp. 602–607.

[10] L. Liu *et al.*, "The COST 2100 MIMO channel model," *IEEE Wireless Commun.*, vol. 19, no. 6, pp. 92–99, 2012.

[11] S. Mukherjee and R. Chopra, "Performance analysis of cell-free massive MIMO systems in LoS/ NLoS channels," *IEEE Trans. Veh. Technol.*, pp. 1–1, 2022.

[12] G. Femenias, F. Riera-Palou, A. Álvarez Polegre, and A. García-Armada, "Short-term power constrained cell-free massive-MIMO over spatially correlated Ricean fading," *IEEE Trans. Veh. Technol.*, vol. 69, no. 12, pp. 15 200–15 215, 2020.

[13] Z. Wang, J. Zhang, B. Ai, C. Yuen, and M. Debbah, "Uplink performance of cell-free massive MIMO with multi-antenna users over jointly-correlated Rayleigh fading channels," *IEEE Trans. Wireless Commun.*, pp. 1–1, 2022.

[14] E. Damosso and L. Correira, "Digital mobile radio: COST 231 view on the evolution towards 3rd generation systems," *Eur. Commission*, 1998.

[15] T. Choi *et al.*, "A realistic path loss model for cell-free massive MIMO in urban environments - modeling approach and experimental results," *to be submitted*, 2022.

[16] R. Wang, M. Shen, Y. He, and X. Liu, "Performance of cell-free massive MIMO with joint user clustering and access point selection," *IEEE Access*, vol. 9, pp. 40 860–40 870, 2021.